PROPERTIES OF POLYAMIDE 6 AND THERMOPLASTIC POLYURETHANE BLENDS CONTAINING MODIFIED MONTMORILLONITES

M. Stankowski[1]*, Anna Kropidłowska[2], Maria Gazda[3] and J. T. Haponiuk[1]

[1]Gdańsk University of Technology, Chemical Faculty, Department of Polymer Technology, G. Narutowicza Str. 11/12
80-952 Gdańsk, Poland
[2]Gdańsk University of Technology, Chemical Faculty, Department of Inorganic Chemistry, G. Narutowicza Str. 11/12
80-952 Gdańsk, Poland
[3]Gdańsk University of Technology, Faculty of Applied Physics and Mathematics, Department of Solid State,
G. Narutowicza Str. 11/12 80-952 Gdańsk, Poland

A series of polyamide 6 nanocomposites (NC) and PA6/TPU/clay nanocomposite blends (NCB) were prepared from commercial polyamide 6, synthesized thermoplastic polyurethanes and two types of organically modified montmorillonites – Cloisite® 10A and Cloisite® 20A.

The thermal behavior was examined by non-isothermal thermogravimetry (TG, DTG), differential scanning calorimetry (DSC) and dynamic-mechanical thermal analysis (DMTA). It has been proved that the thermal stability and tensile properties of these new systems were greater when the organoclay was present within the polymer matrix. What more these properties depend on both the OMMT loading and the type of the gallery cations of organically modified montmorillonites.

Keywords: blend, nanocomposite, polyamide, polyurethane, thermal analysis

Introduction

Polymer nanocomposites (PNC) are inorganic/organic hybrid systems with matrix reinforced using nano-sized particles. For the last two decades these materials have gained great scientific and technological interest. It is caused by the possibility of improving physico-mechanical, thermal and other properties achieved at very low nanoparticle content (<5 mass%) [1]. This characteristic can be exploited to design a more customized composite structure because the lower nanofiller loading results in lighter structural components. The use of nanofillers as modifiers of construction polymers contributed to a considerable development of these systems. The first commercial hybrids, developed in the mid 80's by Toyota research group were polyamide 6 nanocomposites [2] with superior strength, modulus, barrier properties, flame retardancy and heat distortion temperature with respect to pure PA6. The increased dimensional stability has been also determined in these nanocomposites. From that time properties and degradability not only of PA systems [3–6], but as well of various other hybrids [7–15] have been investigated and discussed in the literature.

Lately much attention have been focused also on some nanocomposite blends (NCB), for instance with polyamide matrix [16]. In the case of blends it is possible to change the parameters by simply employing different components. Chow *et al.* [17] were investigating different PA6/PP systems and they obtained compatible blends of relatively high viscosity when organically modified montmorillonite was introduced into the matrix. The best mechanical properties were achieved in the case of 4 mass% addition of silicate. What more, during the studies of PA6/PP/OMMT blends they have also noticed that the nanofiller was present in polyamide matrix [18]. The influence of Cloisite 25A on PA6/LLDPE systems was examined by Yoo *et al.* [19]. This group has received both intercalated and exfoliated nanocomposites, what was confirmed using SEM and X-ray diffraction. All these new systems represent an alternative to conventionally filled polymers or polymer blends in products obtained by melt processing techniques [20–24]. These methods are now of great interest because of the possible advantageous production of the commercial materials.

Recently we have reported on preparation of PA6 nanocomposites and of a new class of PA6 nanocomposite blends [25, 26]. In this paper we characterize these hybrids in the terms of thermal and X-ray analyses. Additionally tensile measurements were performed and water absorption was estimated.

---

*   Author for correspondence: mic@urethan.chem.pg.gda.pl

Experimental

Materials

All nanocomposite systems were obtained using a twin screw extruder from:

- commercial grade polyamide 6 (Tarnamid T-27 MS) [27]
- polyurethanes (TPU) synthesized in our laboratory from poly(ethylene,butylene)adipate diol (PEBA, Poles 55/20, obtained from ZACHEM, Bydgoszcz, Poland); 4,4'-methylene diisocyanate (MDI, obtained from Borsodchem Hungary) and 1,4-butanediol (1,4-BD, purchased from B.A.S.F. Germany). PEBA and 1,4-BD were separately dried by heating at 100°C and stirring under reduced pressure. MDI was melted at 46°C and filtered before use
- appropriate montmorillonite modified with a quaternary ammonium salt (OMMT) Cloisite® 10A or Cloisite® 20A both modified with different quaternary ammonium salts [28] purchased from Southern Clay Products Inc., Texas, USA). OMMT were dried for 6 h at 90°C in a thermal vacuum chamber

Samples prepared for the measurements (Table 1) were moulded by injection and dried for 6 h at 80°C before testing.

Methods

Thermal analysis (TG and DTG curves) was performed using Perkin-Elmer Thermogravimetric Analyzer TGA Pyris 1 at a heating rate of 20°C min^{-1} under nitrogen flow and heating program 25–600°C. DSC measurements were made using Perkin-Elmer Differential Scanning Calorimeter DSC 7 for encapsulated (aluminum pans) samples of ca. 3–10 mg at a heating/cooling rate of 20°C min^{-1} under nitrogen flow. The second melting scan was also performed. The calibration of the temperature and heat flow scales at the

Table 1 Samples designation and formulations

Designation	Composition	Parts/mass%
PA6	PA6	100
NC-I	PA6/Cloisite 10A	98/2
NC-II	PA6/Cloisite 10A	96/4
NC-III	PA6/Cloisite 20A	98/2
NC-IV	PA6/Cloisite 20A	96/4
NCB-I	PA6/TPU/Cloisite 10A	96/2/2
NCB-II	PA6/TPU/Cloisite 10A	92.5/5.5/2
NCB-III	PA6/TPU/Cloisite 10A	90.5/5.5/4
NCB-IV	PA6/TPU/Cloisite 20A	96/2/2
NCB-V	PA6/TPU/Cloisite 20A	92.5/5.5/2
NCB-VI	PA6/TPU/Cloisite 20A	90.5/5.5/4

same heating rate was performed with In and Zn. For the DMTA measurements an analyzer from Polymer Laboratories was used in the bending mode (at 10 Hz frequency and 4°C min^{-1} heating rate). The X-ray patterns of the crystalline residues were recorded in a X'Pert Philips diffractometer (source radiation: CuK$_{\alpha_1}$, λ=0.1546 nm, 40 kV, 30 mA) in the 0.5–10° (2θ range) and at scanning rate 0.25° s^{-1}. Zwick/Roell Z020 testing machine was used to verify mechanical properties of the samples (ISO 527).

Results and discussion

Depending on the interaction between polymer and nanocomposite different structures of hybrids may be formed [29]. Therefore it was necessary to use X-ray diffraction analysis to confirm the formation of the PA6/OMMT nanocomposites and PA6/TPU/OMMT nanocomposite blends. The XRD patterns obtained for the investigated samples are shown in the Fig. 1.

For nanocomposites containing aromatically modified Cloisite® 10A exfoliated structure may be presumed. The diffraction maxima of the montmorillonite are not present (Fig. 1a) indicating that the original crystalline structure of the organoclay is destroyed. This assumption was confirmed also by the rheological and AFM investigations [30].

For the nanocomposites containing aliphatically modified Cloisite® 20A one can observe maxima at lower 2θ values (Fig. 1b) with the intergallery spacing estimated as wide as ca. 1.5–2.0 nm. The results thus showed that the polymer chains penetrate between the layers of the organically modified montmorillonite to form nanocomposites of intercalated structure.

In the case of nanocomposites obtained using semi-crystalline polymer matrix (such as polyamide) the presence of silicate impacts the crystalline structure, since the clay disturbs the formation of hydrogen bonds. Therefore it is always important to characterize all the phases present within this nanoscale system i.e. layered silicate, amorphous and crystalline polymer regions. The results obtained using XRD in width angle region are presented in Fig. 2. We have observed that the 2 mass% addition of clay favored the formation of the γ crystalline phase of polyamide comparing to the pure PA6, what is represented as a peak at 21.3°. In the case of further increase of silicate content (4 mass%) this maximum is still present but the intensity of this peak decreases. Also for the nanocomposite blends diffraction peaks for both α and γ crystalline forms are present at 20.1, 23.5 and 21.3° (2θ), respectively. The α$_2$ peak is a dominant one, while the intensity of the α$_1$ in NC and NCB decreases as suggested by Lincoln *et al.* [31]. In sharp contrast to NC, in nanocomposite blends, the addition of thermoplastic
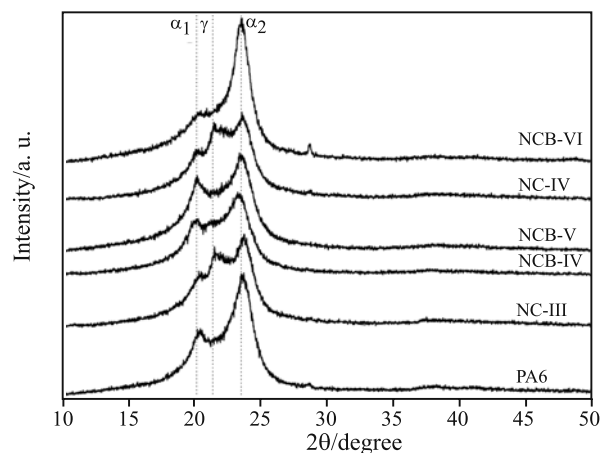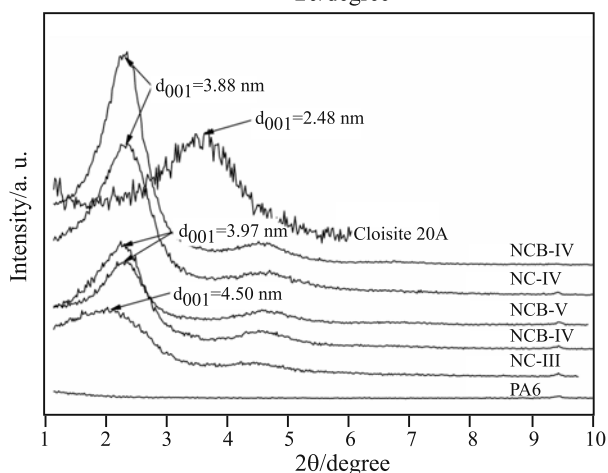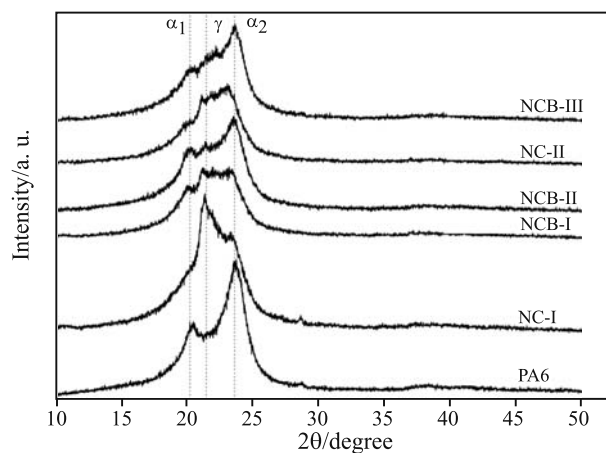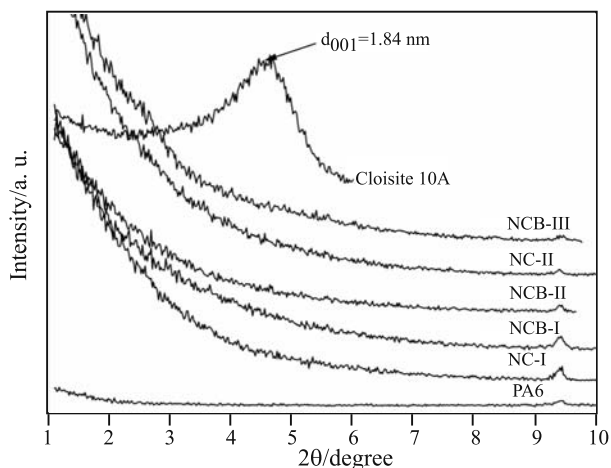
Fig. 1 X-ray diffraction patterns of OMMT (Cloisite® 10A and Cloisite® 20A), nanocomposites (NC) and nano-composites blends (NCB) containing 2 mass% OMMT

Fig. 2 X-ray diffraction patterns of investigated nanocomposites (NC) and nanocomposites blends (NCB)

polyurethane phase caused decrease of γ form content (compare e.g. NC-I and NCB-I) (Fig. 2).

Changes in the crystalline structure of the polyamide 6 caused by the presence of montmorillonite particles in the nanocomposites were observed not only by means of XRD, but also in the DSC measurements. Figure 3 shows DSC curves for virgin PA6, PA6/OMMT nanocomposites and PA6/TPU/OMMT

Table 2 DSC data from for PA6/OMMT nanocomposites and PA6/TPU/OMMT nanocomposite blends

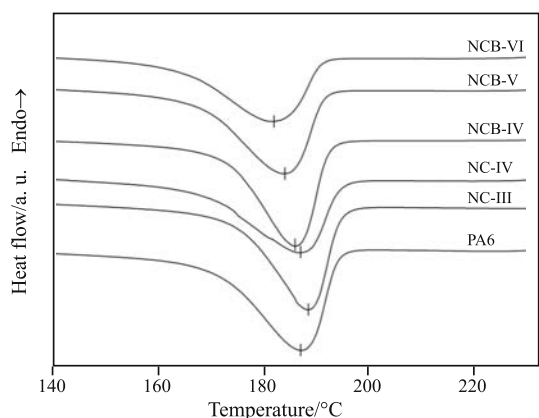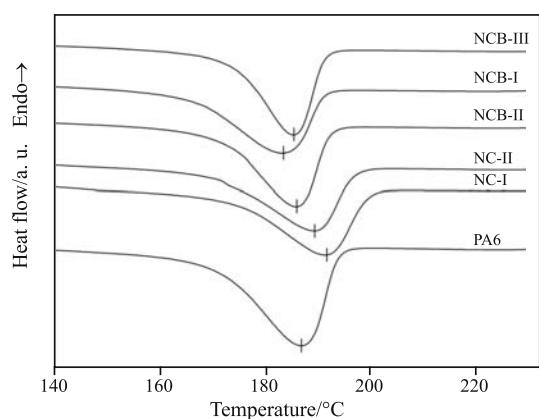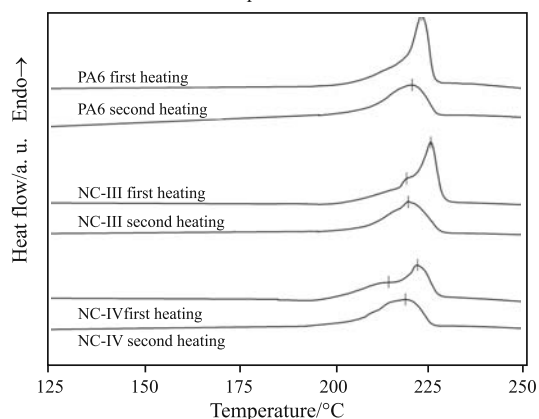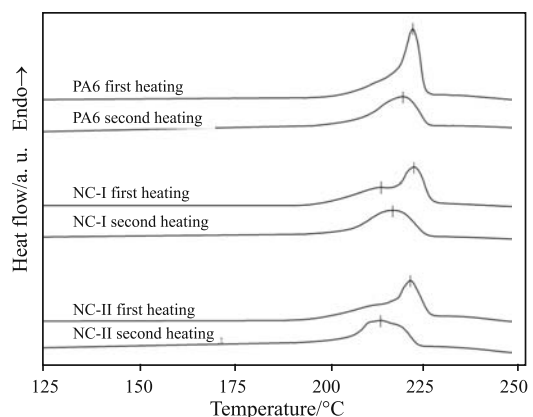| Sample	Heating				Cooling	
	T_{max}/°C 1 scan	ΔH/J g^{-1} 1 scan	T_{max}/°C 2 scan	ΔH/J g^{-1} 2 scan	T_{max}/°C	ΔH/J g^{-1}
PA6	223.0	69.5	220.4	49.9	186.8	−59.7
NC-I	213.7; 223.4	65.5	218.0	49.7	191.8	−43.5
NC-II	213.1; 222.4	56.0	214.5	44.3	189.5	−40.6
NCB-I					185.9	−44.0
NCB-II					183.2	−41.2
NCB-III					185.4	−40.8
NC-III	219.1; 225.4	69.2	219.4	46.1	188.3	−52.2
NC-IV	213.1; 221.7	57.8	218.9	46.5	186.8	−47.6
NCB-IV					185.7	−53.1
NCB-V					183.6	−50.1
NCB-VI					181.7	−42.3

Fig. 3 The DSC heating and cooling curves for virgin PA6, PA6 nanocomposites (NC) and PA6/TPU/OMMT nanocomposite blends (NCB)
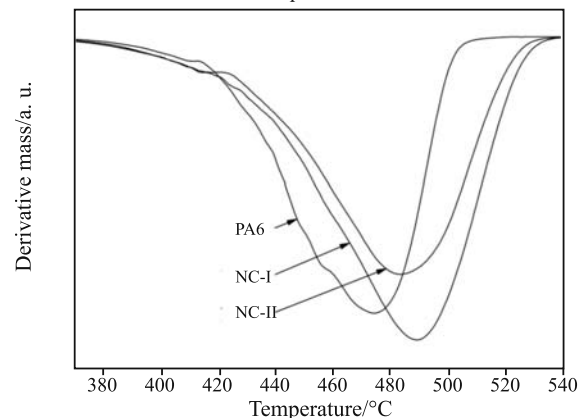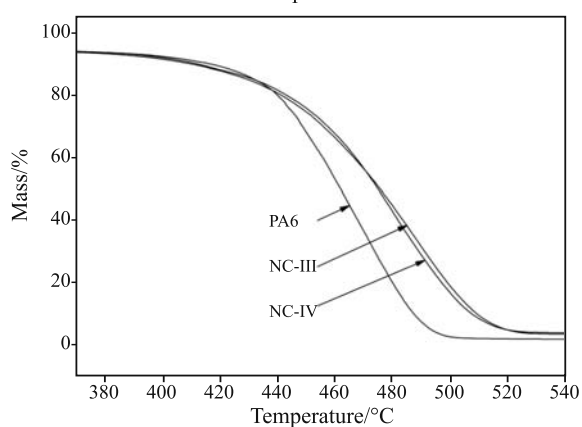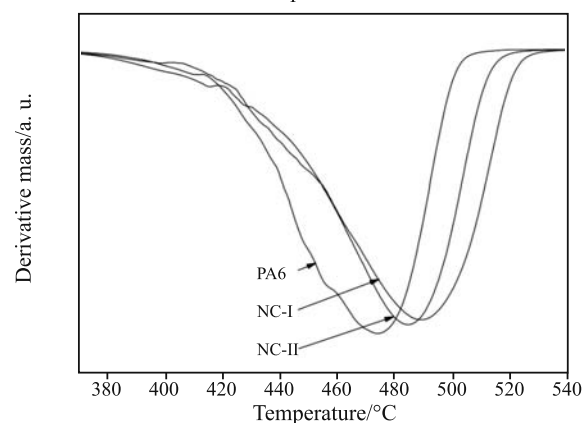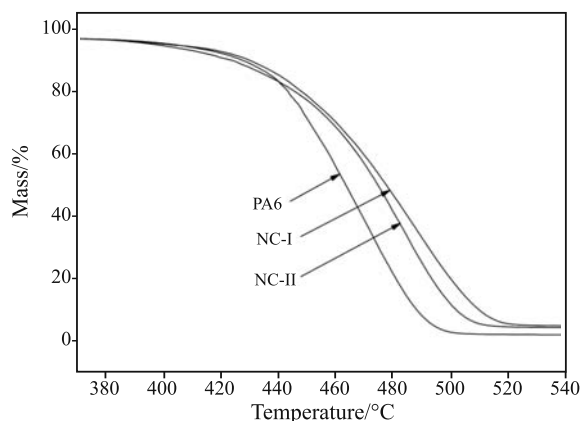

Fig. 4 TG and DTG curves for virgin PA6 and PA6 nanocomposites with different type and loading of OMMT

Table 3 Temperatures for 10 and 50% mass loss and the temperature of the maximal decomposition rate estimated for PA6 nanocomposites

Sample	Temperature/°C		T_{dmax}/°C
	10	50	
PA6	425.5	462.7	474.0
NC-I	428.5	477.0	490.1
NC-II	421.1	474.2	485.3
NC-III	421.2	476.8	489.7
NC-IV	422.1	476.1	484.4

nanocomposite blends. The related data are presented in the Table 3.

The α-PA6 form is dominant and characterized by the melting peak at 223°C, which position is not substantially influenced by the nanofiller, however an increase of γ-PA6 form content (melting peak at 213°C) can be also seen. The maximal crystallization rate occurs for the nanocomposites at higher temperatures than for virgin PA6, but in the case of polymer nanocomposite blends (lower crystallinity degree of the PA6 component observed), the elastomeric component TPU shifts the temperature of maximal crystallization rate to lower values. It is possible that the OMMT particles can act as heterogeneous nuclei [32], shifting the position of the crystallization peak to the higher temperatures. On the contrary, blending thermoplastic polyurethane with polyamide 6, causing lowering of the crystallization temperature [33]. The observed crystallization behaviour of PA6/TPU/OMMT nanocomposite blends origins from overlapping of the counterbalancing influences of the elastomer and the nanofiller.

The results obtained for the PA6 and the nanocomposites using thermogravimetric analysis (TG) are presented in Fig. 4 and Table 3.

Polyamide 6 nanocomposites obtained using either Cloisite® 10A or Cloisite® 20A exhibit better thermal stability comparing with the virgin polyamide 6 (Fig. 3). Because of the interfacial interactions and the montmorillonite-polymer multilayered nanoscale organization the thermal decomposition peaks are shifted towards higher temperatures. At low nanoparticle loading the stability improvement was observed up to 2 mass% of the montmorillonite.

The results obtained using dynamic-mechanical thermal analysis (DMTA) curves for PA6/OMMT nanocomposites (NC) and PA6/TPU/OMMT nanocomposites blends (NCB), containing 2 and 4 mass% organically modified montmorillonite are presented in Fig. 5 and Table 4.

Comparing to the polyamide 6, the dynamic storage modulus of the PA6 nanocomposites and nanocomposite blends is higher in the temperature ranges below and above the glass transition. It is im-
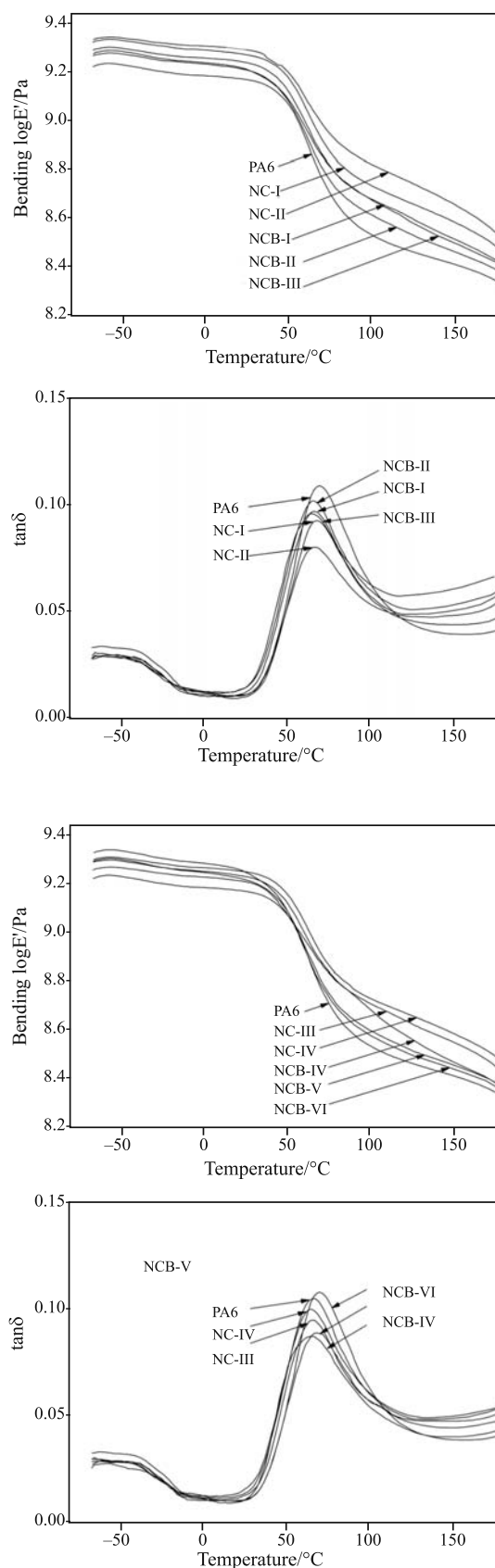

Fig. 5 Comparison of the DMTA behavior of virgin PA6, PA6 nanocomposites (NC) and PA6 nanocomposite blends (NCB)

Table 4 Glass transition temperature and storage moduli (values at 0 and 100°C) of virgin PA6, PA6 nanocomposites and PA6 nanocomposite blends

| Sample	PA6	NC-I	NC-II	NCB-I	NCB-II	NCB-III	NC-III	NC-IV	NCB-IV	NCB-V	NCB-VI
$T_g \, \delta$/°C	68.8	67.0	65.6	65.6	64.9	63.5	63.0	67.4	64.5	64.5	64.3
log$E$'/GPa at 0°C	1.51	1.93	2.01	1.80	1.72	1.70	1.68	1.83	1.77	1.75	1.91
log$E$'/MPa at 100°C	338	544	660	478	407	472	510	536	483	397	360

Table 5 Physico-mechanical properties of virgin PA6, PA6/OMMT nanocomposites (NC) and PA6/TPU/OMMT nanocomposite blends (NCB)

Sample	Yield stress/MPa	Strain at brake/%	Density/g cm^{-3}	Hardness/°Shore D	H_2O absorption (24 h)/%
PA6	64.1	199.0	1.13	73.6	2.26
NC-I	79.9	74.7	1.14	75.3	1.26
NC-II	86.1	52.4	1.15	76.2	1.11
NCB-I	73.5	254.2	1.14	74.3	1.24
NCB-II	64.1	278.3	1.16	72.4	1.28
NCB-III	66.8	146.1	1.16	74.0	1.16
NC-III	78.1	84.4	1.15	74.0	1.24
NC-IV	71.3	58.3	1.16	75.0	1.18
NCB-IV	66.3	143.4	1.15	73.7	1.23
NCB-V	56.9	328.5	1.15	72.0	1.32
NCB-VI	59.1	170.1	1.16	71.8	1.25

portant to note the enhanced storage modulus of nanocomposite systems at temperatures above room temperature. NC-II (E'=660 MPa at 100°C) possess the storage modulus twice as big as the pure polyamide 6 (E'=338 MPa at 100°C). The addition of the thermoplastic polyurethane caused decrease of E' compared to polyamide nanocomposites (NC) nevertheless NCB (see e.g. nanocomposite obtained using 4 mass% montmorillonite) in comparison with PA6 exhibit higher values of storage modulus, in entire temperature range. The glass transition temperature of the PA6 nanocomposites is slightly lowered comparing to the PA6. More distinct shift to the lower temperatures is observed for the TPU containing nanocomposite blends (Table 4).

The influence of the OMMT and TPU on the tensile characteristics of the investigated nanocomposites and nanocomposite blends is shown in Fig. 6.

The yield stress estimated for the nanocomposites and for the majority of the nanocomposite blends is significantly enhanced over the value for the virgin PA6. For the NC-II the maximal stress is 22 MPa higher than the value recorded for the pure PA6. The strain at break of the PA6/OMMT nanocomposites is reduced and in the case of the PA6/TPU/OMMT nanocomposite blends, due to the elastomer content, visibly enlarged comparing with the polyamide 6 (Fig. 6). Water absorption data for the investigated nanocomposites and nanocomposite blends was twice as low as for the virgin PA6 (Ta-
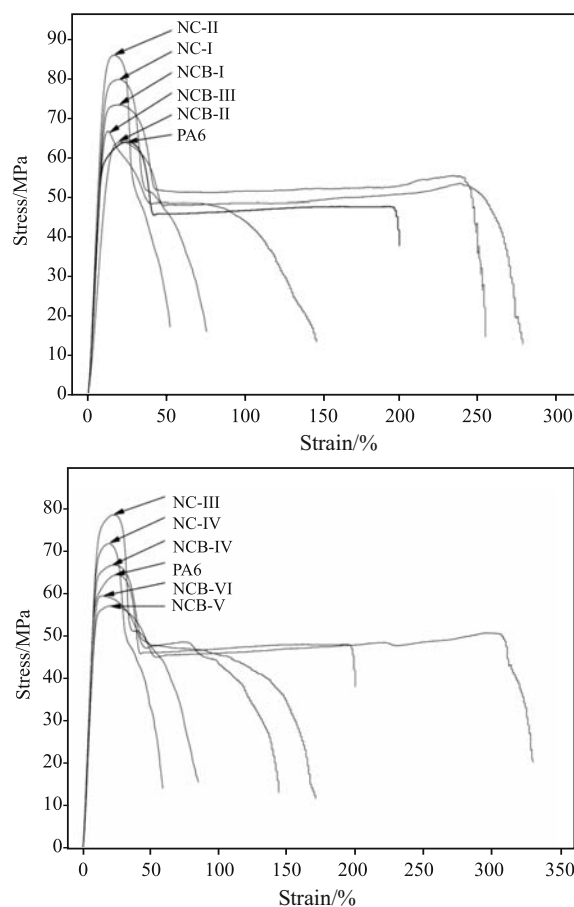
Fig. 6 Stress *vs.* strain for PA6/OMMT nanocomposites (NC) and PA6/TPU/OMMT nanocomposite blends (NCB)

ble 5). Reduction in the gas and liquid permeability is usually attributed to the fact that the diffusing molecules have to bypass the impermeable silicate platelets (labyrinth effect) which are more or less well oriented normal to the diffusion direction [34]. As expected, the nanofiller enhanced also the hardness of PA6/OMMT nanocomposites (Table 5). The reverse effect of the TPU phase in the PA6/TPU/OMMT nanocomposite blends resulted in smaller hardness differences in relation to the virgin PA6.

Conclusions

Structure and properties of PA6/OMMT nanocomposites and PA6/TPU/OMMT nanocomposite blends were investigated using two kinds of (aromatically and aliphatically modified) montmorillonites. The addition of clay caused formation exfoliated or intercalated structures. In both cases improvement in thermal and tensile properties was estimated. The strengthening of the amorphous phase is represented by the increase of the dynamic storage modulus above the glass transition. Particularly the investigated PA6/TPU blends were advantageously modified by the nanofiller, exhibiting at the same time improvement in yield stress, elasticity and thermal stability.

Acknowledgements

References

1 Y. May and Z. Yu, Eds, Polymer Nanocomposites, Woodhead Publishing Ltd., England 2006.
2 US patent 4,739,007; 1988.
3 S. Wang, Y. Hu, Z. Li, Z. Wang, Y. Zhuang, Z. Chen and W. Fan, Colloid. Polym. Sci., 281 (2003) 951.
4 G. Srinath and A. R. Gnanamoorthy, J. Mater. Sci., 40 (2005) 2897.
5 J. S. Chois, S. T. Lim and H. J. Choi, J. Mater. Sci., 41 (2006) 1843.
6 W. S. Chow and Z. A. Mohd Ishak, eXPRESS Polym. Lett., 1 (2007) 77.
7 R. Kotsilkova, V. Petkova and Y. Pelovski, J. Therm. Anal. Cal., 64 (2001) 591.
8 W. B. Xu, Z. F. Zhou, M. L. Ge and W.-P. Pan, J. Therm. Anal. Cal., 78 (2004) 91.
9 J. Xiao, Y. Hu, Q. Kong, L. Song, Z. Wang, Z. Chen and W. Fan, Polym. Bull., 54 (2005) 271.
10 A. Cheng, S. Wu, D. Jiang, F. Wu and J. Shen, Colloid. Polym. Sci., 284 (2006) 1057.
11 M. Day, A. V. Nawaby and X. Liao, J. Therm. Anal. Cal., 86 (2006) 623.
12 M. A. Kader, A. K. Kim, A. Y.-S. Lee and A. C. Nah, J. Mater. Sci., 41 (2006) 7341.
13 V. Causin, C. Marega, R. Saini, A. Marigo and G. Ferrara, J. Therm. Anal. Cal. (2007), OnlineFirst.
14 M. A. Treece and J. P. Oberhauser, Macromolecules, 40 (2007) 571.
15 M. Kráčalík, J. Mikešová, R. Puffr, J. Baldrian, R. Thomann and Ch. Friedrich, Polym. Bull., 58 (2007) 313.
16 S. C. Tjong, Y. Z. Meng and Y. Xu, J. Appl. Polym. Sci., 86 (2002) 2330.
17 W. S. Chow, Z. A. Mohd Ishak and J. Karger-Kocsis, Macromol. Mater. Eng., 290 (2005) 122.
18 W. S. Chow, Z. A. Mohd Ishak and J. Karger-Kocsis, J. Polym. Sci., 43 (2005) 1198.
19 Y. Yoo, Ch. Park, S.-G. Lee, K.-Y. Choi, D. S. Kim and J. H. Lee, Macromol. Chem. Phys., 206 (2005) 878.
20 Ch. Ding, B. Guo, H. He, D. Jia and H. Hong, Eur. Polym. J., 41 (2005) 1781.
21 T. J. Pinnavaia and G. W. Beall, Polymer-Clay Nanocomposites, Wiley, Chichester 2000.
22 G. H. Michler and F. J. Balta-Calleja, Mechanical Properties of Polymer Based on Nanostructure and Morphology, Taylor & Francis, 2005.
23 S. Sinha Ray and M. Okamoto, Progr. Polym. Sci., 28 (2003) 1593.
24 L. Chazeau, C. Gauthier, G. Vigier and J. Y. Cavaille, Handbook of Organic-Inorganic Hybrid Materials and Nanocomposites, Vol. 2: Nanocomposites, American Scientific Publ., 2003.
25 M. Strankowski, J. T. Haponiuk, M. Gazda and H. Janik, e-polymers, Conference Papers, Intern. Polymer Seminar Gliwice 2005, http://www.e-polymers.org.
26 M. Strankowski, Ph.D. Dissertation, Gdańsk University of Technology 2006.
27 Tworzywa sztuczne commercial directory by Zakłady Azotowe w Tarnowie Mościcach S.A. (2002).
28 Product Bulletin by Clay Products, Inc., available online: http://www.scprod.com
29 L. A. Utracki, Clay-Containing Polymeric Nanocomposites, Rapra Technology Ltd., UK 2004.
30 M. Strankowski, J. T. Haponiuk, G. Nowaczyk and M. Gazda, Ann. Pol. Chem. Soc., (2007) 561.
31 D. M. Lincoln, R. A. Vaia, Z. G. Wang and B. S. Hsiao, Polymer, 42 (2001) 1621.
32 W. B. Xu, H. B. Zhai, H. Y. Guo, Z. F. Zhou, N. Whiteley and W.-P. Pan, J. Therm. Anal. Cal., 78 (2004) 101.
33 J. T. Haponiuk, J. Therm. Anal. Cal., 60 (2000) 45.
34 P. M. Ajayan, L. S. Schadler and P. V. Braun, Eds, Nanocomposite Science and Technology, Wiley-VCH Verlag, Weinheim 2003.